Optical ridge waveguides in 4H-SiC single crystal produced by combination of carbon ion irradiation and femtosecond laser ablation

Qingfang Luan,[1] Yuechen Jia,[1] Yutian Wang,[2] Shavkat Akhmadaliev,[2] Shengqiang Zhou,[2] Javier R. Vázquez de Aldana,[3] Yang Tan,[1] and Feng Chen[1,*]

[1]*School of Physics, Key Laboratory of Particle Physics and Particle Irradiation (Ministry of Education), and State Key Laboratory of Crystal Materials, Shandong University, Jinan 250100, China*

[2]*Helmholtz-Zentrum Dresden - Rossendorf, Institute of Ion Beam Physics and Materials Research, Bautzner Land Strasse 400, Dresden 01328, Germany*

[3]*Laser Microprocessing Group, Universidad de Salamanca, Salamanca 37008, Spain*

[*]*drfchen@sdu.edu.cn*

Abstract: Optical ridge waveguides were fabricated in 4H-SiC single crystal by combination of 15 MeV C^{5+} ion irradiation and femtosecond laser ablation. The near-field modal intensity distributions exhibit the well-confined light propagation in the waveguides. A propagation loss as low as 5.1 dB/cm has been achieved at 632.8 nm for the ridge waveguide. The investigation of confocal micro-Raman spectra suggests partial transition of 4H-SiC to 6H-SiC in the irradiated region.

OCIS codes: (230.7370) Waveguides; (140.3390) Laser materials processing; (160.6000) Semiconductor materials.

References and links

1. R. J. Trew, J.-B. Yan, and P. M. Mock, "The potential of diamond and SiC electronic devices for microwave and millimeter-wave power applications," Proc. IEEE **79**(5), 598–620 (1991).
2. M. Bhatnagar and B. J. Baliga, "Comparison of 6H-SiC, 3C-SiC, and Si for power devices," IEEE Trans. Electron. Dev. **40**(3), 645–655 (1993).
3. Y. Shoji, K. Nakanishi, Y. Sakakibara, K. Kintaka, H. Kawashima, M. Mori, and T. Kamei, "Hydrogenated amorphous silicon carbide optical waveguide for telecommunication wavelength applications," Appl. Phys. Express **3**(12), 122201 (2010).
4. K. Ito, S. Tsukimoto, and M. Murakami, "Effects of Al ion implantation to 4H-SiC on the specific contact resistance of TiAl-based contact materials," Sci. Technol. Adv. Mater. **7**(6), 496–501 (2006).
5. S. Doğan, A. Teke, D. Huang, H. Morkoc, C. B. Roberts, J. Parish, B. Ganguly, M. Smith, R. E. Myers, and S. E. Saddow, "4H-SiC photoconductive switching devices for use in high-power applications," Appl. Phys. Lett. **82**(18), 3107–3109 (2003).
6. R. S. Wei, S. Song, K. Yang, Y. X. Cui, Y. Peng, X. F. Chen, X. B. Hu, and X. G. Xu, "Thermal conductivity of 4H-SiC single crystals," J. Appl. Phys. **113**(5), 053503 (2013).
7. L. Li, W. Hua, S. Prucnal, S. D. Yao, L. Shao, K. Potzger, and S. Q. Zhou, "Defect induced ferromagnetism in 4H-SiC single crystals," Nucl. Instrum. Methods Phys. Res. B **275**, 33–36 (2012).
8. H. Y. Sun, S. C. Lien, Z. R. Qiu, H. C. Wang, T. Mei, C. W. Liu, and Z. C. Feng, "Temperature dependence of Raman scattering in bulk 4H-SiC with different carrier concentration," Opt. Express **21**(22), 26475–26482 (2013).
9. S. C. Hong, M. J. Zhan, G. Wang, H. W. Xuan, W. Zhang, C. J. Liu, C. H. Xu, Y. Liu, Z. Y. Wei, and X. L. Chen, "4H-SiC: a new nonlinear material for mid infrared lasers," Laser Photon. Rev. **7**(5), 831–838 (2013).
10. F. Chen, "Micro- and submicrometric waveguiding structures in optical crystals produced by ion beams for photonic applications," Laser Photon. Rev. **6**(5), 622–640 (2012).
11. G. Pandraud, E. Margallo-Balbas, C.-K. Yang, and P. J. French, "Experimental characterization of roughness induced scattering losses in PECVD SiC waveguides," J. Lightwave Technol. **29**(5), 744–749 (2011).
12. G. Pandraud, P. J. French, and P. M. Sarro, "Experimental study of bent SiC optical waveguides," Microw. Opt. Technol. Lett. **47**(3), 219–220 (2005).
13. S. Sorieul, X. Kerbiriou, J.-M. Costantini, L. Gosmain, G. Calas, and C. Trautmann, "Optical spectroscopy study of damage induced in 4H-SiC by swift heavy ion irradiation," J. Phys. Condens. Matter **24**(12), 125801 (2012).
14. M. Ishimaru, R. M. Dickerson, and K. E. Sickafus, "High-dose oxygen ion implantation into 6H-SiC," Appl. Phys. Lett. **75**(3), 352 (1999).
15. W. Wesch, A. Heft, R. Menzel, T. Bachmann, G. Peiter, H. Hobert, T. Höche, P. Dannberg, and A. Bräuer, "Ion beam processing of SiC for optical application," Nucl. Instrum. Methods Phys. Res. B **148**(1–4), 545–550 (1999).

#208123 - $15.00 USD Received 13 Mar 2014; revised 4 May 2014; accepted 6 May 2014; published 12 May 2014

16. F. Chen and J. R. Vázquez de Aldana, "Optical waveguides in crystalline dielectric materials produced by femtosecond-laser micromachining," Laser Photon. Rev. **8**(2), 251–275 (2014).
17. R. Degl'Innocenti, S. Reidt, A. Guarina, D. Rezzonico, G. Poberaj, and P. Gunter, "Micromachining of ridge optical waveguides on top of He-implanted β-BaB_2O_4 crystals by femtosecond laser ablation," J. Appl. Phys. **100**(11), 113121 (2006).
18. R. Ramponi, R. Osellame, and M. Marangoni, "Two straightforward methods for the measurement of optical losses in planar waveguides," Rev. Sci. Instrum. **73**(3), 1117–1121 (2002).
19. C. Zhang, N. N. Dong, J. Yang, F. Chen, J. R. Vázquez de Aldana, and Q. M. Lu, "Channel waveguide lasers in Nd:GGG crystals fabricated by femtosecond laser inscription," Opt. Express **19**(13), 12503–12508 (2011).
20. J. F. Ziegler, computer code, SRIM *http://www.srim.org*.
21. http://www.rsoftdesign.com.
22. D. Yevick and W. Bardyszewski, "Correspondence of variational finite-difference (relaxation) and imaginary-distance propagation methods for modal analysis," Opt. Lett. **17**(5), 329–330 (1992).
23. Y. C. Yao, Y. Tan, N. N. Dong, F. Chen, and A. A. Bettiol, "Continuous wave Nd:YAG channel waveguide laser produced by focused proton beam writing," Opt. Express **18**(24), 24516–24521 (2010).
24. H. Y. Sun, F. He, Z. H. Zhou, Y. Cheng, Z. Z. Xu, K. Sugioka, and K. Midorikawa, "Fabrication of microfluidic optical waveguides on glass chips with femtosecond laser pulses," Opt. Lett. **32**(11), 1536–1538 (2007).
25. A. Vonsovici, G. T. Reed, A. G. R. Evans, and F. Namavar, "Loss measurements for β-SiC-on insulator waveguides for high-speed silicon-based photonic devices," Proc. SPIE **3630**, 115–124 (1999).
26. S. Sorieul, J.-M. Costantini, L. Gosmain, L. Thomé, and J.-J. Grob, "Raman spectroscopy study of heavy-ion-irradiated α-SiC," J. Phys. Condens. Matter **18**(22), 5235–5251 (2006).
27. L. Li, S. Prucnal, S. D. Yao, K. Potzger, W. Anwand, A. Wagner, and S. Q. Zhou, "Rise and fall of defect induced ferromagnetism in SiC single crystals," Appl. Phys. Lett. **98**(22), 222508 (2011).

1. Introduction

As one of the most favorite third-generation semiconductors, silicon carbide (SiC) has attracted considerable attentions owing to its intriguing features, such as high thermal conductivity (~4.5 W/cm·K), high electric field breakdown strengths (~3×10^6 V/cm), and large band gap (~3 eV), for applications in high-power electronic devices of many fields, e.g., microelectronics, microwaves, aerospace, and nuclear reactor system to radar communication, etc [1–5]. The 4H-SiC, a member of SiC family, has a hexagonal structure and exists in a uniaxial crystal formed at the temperature above 1700°C. It has been widely used in the manufacturing of electronic devices which are of high frequency, enhanced power, and good radiation or interference resistance dependence [4]. The properties of 4H-SiC crystals on thermal conductivity [6], ferromagnetism [7], and Raman scattering [8] have been investigated by a few groups. More recently, the 4H-SiC has shown its intriguing features as a new nonlinear material for mid-infrared lasers [9].

As the basic elements of integrated photonics, optical waveguides enable the confinement of light fields within small volumes. Consequently, high optical intensities can be achieved due to the compressed light fields inside the waveguide [10]. For 4H-SiC crystals, the physical properties (e.g., Mohs hardness as high as 9.5) and stable chemical stability make it difficult to be directly modified by normal waveguide fabrication techniques. As of yet, SiC waveguides have been produced by PECVD [11, 12], which was not a direct-modify solution of the single crystals, and superior photoelectric devices were implemented for applications in various aspects (i.e., micro-electronics, metallurgy). The ion implantation/irradiation has been proved to be an efficient technique for micromachining of SiC crystals [13–15]. Compared with planar or slab waveguides, the ridge waveguides offer two-dimensional confinement of light fields, which are more appropriate for the construction of compact devices. In addition, considering the high hardness of SiC, the femtosecond (fs) laser ablation seems to be an ideal method for ridge patterning, which has been successfully utilized to manufacture ridge structures on a number of planar waveguides [16, 17].

In this work, we implement the fabrication of the ridge waveguides in 4H-SiC single crystal by combination of carbon ion irradiation and fs laser ablation. Properties of the waveguides such as refractive index profiling, guiding properties, and micro-Raman (μ-Raman) spectroscopy have been investigated in details.

#208123 - $15.00 USD Received 13 Mar 2014; revised 4 May 2014; accepted 6 May 2014; published 12 May 2014

2. Experiments

The 4H-SiC single crystal (oriented along (0001) direction) used in this work was cut into the dimension of 0.4 × 4 × 10 mm^3 and optically polished. During the experiment, the C^{5+} ions were irradiated into one of the biggest facet (4 × 10 mm^2) at energy of 15 MeV and fluence of 2 × 10^{14} ions/cm^2 to produce a planar waveguide layer by the 3 MV tandem accelerator at Helmholtz-Zentrum Dresden-Rossendorf, Germany. On the irradiated surface (i.e., the planar waveguide), the ridge waveguides were micromachined using the laser facility of the Universidad de Salamanca. A Ti:Sapphire laser system (Spitfire, Spectra Physics), which delivered 120 fs pulses, linearly polarized at 796 nm and with a repetition rate of 1 kHz was used as laser source. The sample was placed in a computer controlled motorized 3-axis stage with a spatial resolution of 0.2 μm. The laser beam was focused at the largest sample surface through a 20 × microscope objective (N.A. ~0.40) and the sample was scanned at a translation velocity of 25 μm/s. Both single-scan and multi-scan technology with different energy (2.0 μJ and 1.2 μJ) were utilized to ablate parallel grooves. As a consequence, the ridge waveguides were fabricated in 4H-SiC crystal with the vertical confinement of the ion irradiated planar waveguide and the lateral restriction of two parallel air grooves, which were ablated with a transverse separation of ~20 μm.

As to investigate the characteristics of the waveguide, the modal profiles of guided modes were investigated by an end-face coupling arrangement at a wavelength of 632.8 nm. The propagation losses of the waveguides were measured along different polarization of probe light through the back-reflection method [18]. The refractive index distributions of the waveguide were reconstructed by the method described in [19]. Moreover, the wavelength range of the guidance of the waveguides was measured by a continuous wave Ti:Sapphire laser (Coherent MBR PE, wavelength ranging from 700 to 960 nm) using the end-face coupling system. A spherical convex lens with focus length of 25 mm was utilized to couple the laser beam into the waveguide. The output light was collected by a 20 × microscope objective lens (N.A. ~0.40) and characterized by a CCD camera and a spectrometer.

In order to study the microstructural changes induced by the 15 MeV C^{5+} ion irradiation, the μ-Raman spectra were measured by a confocal Raman spectrometer (Horiba/Jobin Yvon HR800) at room temperature. During the experiment, a continuous wave laser at wavelength of 473 nm was focused onto the end facet of the sample. With the diameter of the focused beam less than 1μm, the Raman spectra of the waveguide region (about 4 μm beneath the surface) and the bulk were detected, respectively. All the spectral scans were performed in the range of 150~1500 cm^{-1}.

3. Results and discussion

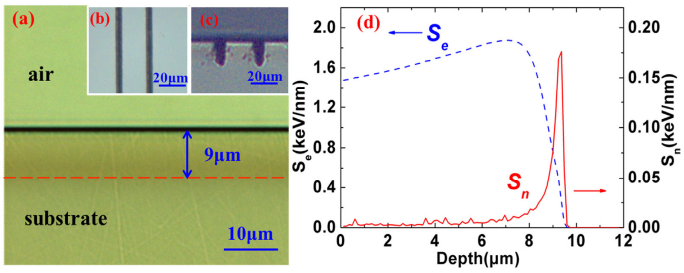

Fig. 1. (a) Optical microscope image of the cross section of the 4H-SiC planar waveguide, the (b) top view, and (c) cross section of the ridge waveguide produced by fs laser ablation, (d) electronic (dashed line) and nuclear (solid line) stopping powers as a function of the depth from the sample surface of the 4H-SiC waveguide.

Figure 1(a) shows the cross-sectional microscopic photograph of the 15 MeV C^{5+} ion irradiated 4H-SiC planar waveguide, which was achieved by a polarized microscope (Axio Imager, Carl Zeiss). It can be seen that the thickness of the ion beam modified section is ~9

#208123 - $15.00 USD Received 13 Mar 2014; revised 4 May 2014; accepted 6 May 2014; published 12 May 2014

μm. That is, indeed, in a good agreement with the projected range of the 15 MeV C^{5+} ions in 4H-SiC crystal calculated by the Stopping and Range of Ions in Matter (SRIM-2011) code [20]. Figures 1(b) and 1(c) exhibit the microscope images of the ridge waveguide with the width of 20 μm produced by the fs laser ablation on the top and cross-sectional views, respectively. Figure 1(d) depicts the electronic (S_e) and the nuclear stopping powers (S_n) of the 15 MeV C^{5+} ions as the function of penetration depth inside the 4H-SiC crystal. From S_e and S_n curves, it is clearly seen that the waveguide thickness is in good agreement with the mean projected range of 15 MeV C^{5+} ions inside 4H-SiC crystal. And the maximum value of S_e is ~1.85 keV/nm, which seems to be too low to generate enough electronic damage for effective refractive index changes [17].

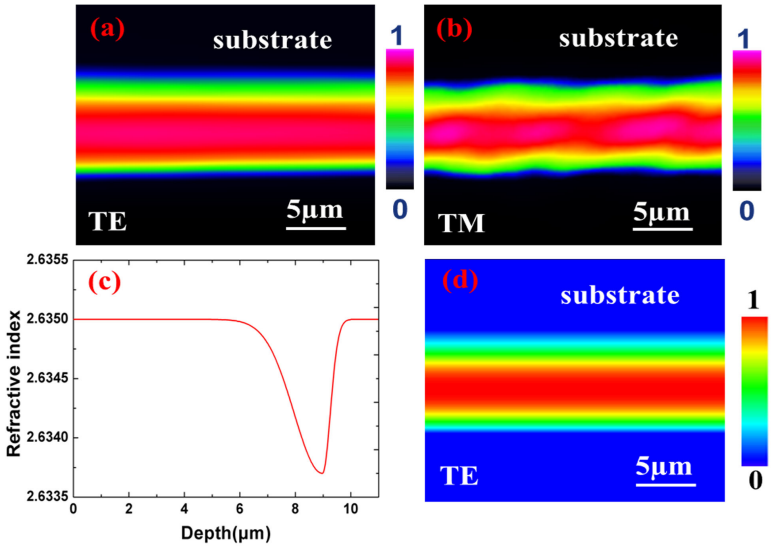

Fig. 2. Measured modal profiles of the 4H-SiC planar waveguide for TE (a) and TM (b) polarizations at 632.8 nm. Reconstructed refractive index profile (c) and calculated modal profile (d) for TE polarization.

In order to characterize only the refractive index change produced by the ion implantation process, the refractive index distribution was constructed by the measured modal profiles. Figures 2(a) and 2(b) are the experimentally measured waveguide modal profiles of planar waveguide in 4H-SiC crystal at TE (Transverse Electric) and TM (Transverse Magnetic) polarizations of detecting light at wavelength of 632.8 nm. Our experiments further show that the 15 MeV C^{5+} irradiated 4H-SiC waveguide supports guidance till wavelength of ~900 nm. Figure 2(c) shows the reconstructed ordinary refractive index profile at 632.8 nm. As one can see, there was a refractive index decrease $\Delta n \approx -1.3 \times 10^{-3}$ at the end of incident ions' trajectory, acting as a typical "optical barrier" with negative index change, meanwhile the refractive index of the surface region remained unchanged. This was confirmed by the *m*-line data (not shown here for brevity). Compared with Fig. 2(c) and Fig. 1(d), it is reasonable to conclude that the nuclear damage plays dominant role on the waveguide construction. Figure 2(d) shows the calculated modal distribution of the planar waveguide by the finite-difference beam propagation method (FD-BPM) with the software Rsoft [21, 22]. From the comparison of the two modal distributions in Figs. 2(c) and 2(d), we can conclude a fairly good agreement between the calculated and experimented modal profiles for 4H-SiC planar waveguide, which suggests that the reconstructed refractive index profile is reasonable.

#208123 - $15.00 USD Received 13 Mar 2014; revised 4 May 2014; accepted 6 May 2014; published 12 May 2014

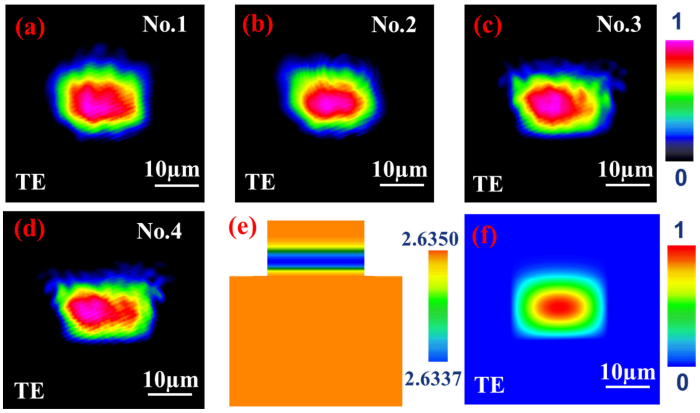

Fig. 3. Measured modal profiles related to TE_{00} of ridge waveguides Nos. 1-4 (a, b, c, and d) at 632.8 nm. Reconstructed refractive index profile (e) and calculated modal profile (f) of waveguide No. 1 along TE polarization.

In order to compare the guiding properties of ridge waveguides with diverse dimensions fabricated by different fs-laser ablation parameters (i.e., different scan numbers and pulse energies, etc.), we fabricated four ridge waveguides labeling No. 1, No. 2, No. 3 and No. 4 (ablation parameters seen in Table 1). Figures 3(a)-3(d) depict the measured mode profiles of ridge waveguide related to TE_{00} with Nos. 1-4, respectively, at 632.8 nm. Similar near-field intensity distributions have been obtained for the TM polarized modes (not presented here for the purpose of brevity). The maximum index modification along the vertical direction in the waveguide layer (i.e., the index contrast between the waveguide core and bulk) was calculated to be $\Delta n \approx 1.28 \times 10^{-3}$ by using the formula

$$\Delta n = \frac{\sin^2 \Theta_m}{2n} \tag{1}$$

where Θ_m is the maximum incident angular deflection at which no transmitted power change occurs, and $n = 2.6350$ is the refractive index of the unmodified substrate [23], which is in good agreement with that obtained from the refractive index reconstruction. The 2D refractive index profile of the ridge waveguide was therefore constructed [Fig. 3(e)]. Based on this index profile, the modal profile of the ridge waveguide is calculated, shown in Fig. 3(f).

Table 1. Propagation losses of planar and ridge waveguides at 632.8 nm

Waveguides	Ablation parameters		Propagation Loss (dB/cm)	
	Scan numbers	Pulse energy (μJ)	TE	TM
Planar	-	-	4.5	5.0
No. 1	1	2.0	5.1	5.8
No. 2	4	2.0	7.2	7.7
No. 3	1	1.2	6.4	7.1
No. 4	4	1.2	8.1	8.8

The propagation losses of the 15 MeV C^{5+} ion irradiated 4H-SiC planar waveguide and ridge waveguides are also shown in Table 1. As one can see, the fs laser micromachined ridge waveguides have higher propagation losses than planar waveguide. The higher attenuation for ridge waveguides should be partly attributed to the roughness of the side-walls fabricated by the fs laser ablation (with typically roughness of more than 2μm). The ridge waveguide of No. 1 fabricated by single-scan technique with pulse energy 2.0 μJ has the lowest propagation loss (~5.1 dB/cm) at TE polarization. From this it can be concluded that with single scan technology the roughness of sidewalls is less than that of multiple scanned sample in 4H-SiC,

#208123 - $15.00 USD Received 13 Mar 2014; revised 4 May 2014; accepted 6 May 2014; published 12 May 2014

which is different from the fs-laser micromachined glass chips [24]. In addition, the relatively high loss values of the planar and ridge waveguides are mainly also due to the light leaky effect through the optical-barrier, which happens often in typical optical-barrier type ion implanted waveguides [10]. Nevertheless, the SiC waveguides in the present work possess lower propagation losses applied in the semiconductor devices compared with the previous work [25], in which propagation loss was estimated as high as ~14.4 dB/cm.

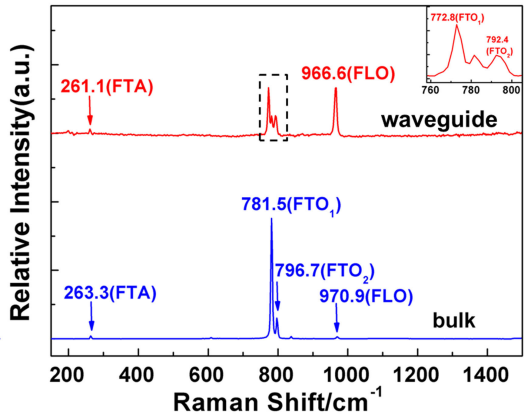

Fig. 4. Confocal micro-Raman spectra obtained from the waveguide region (red) and the bulk (blue) of the 4H-SiC. The inset shows the magnification of the region marked by dashed line.

The Raman spectra of the waveguide and bulk are depicted in Fig. 4. As one can see, the typical peaks of ~263.3 (FTA), ~781.5 (FTO_1), ~796.7 (FTO_2) and ~970.9 cm^{-1} (FLO) are observed at the bulk of 4H-SiC. Compared with the bulk, Raman peak positions of the waveguide region shift to lower wave numbers and the intensity at FTO mode is weaker. The decrease of relative Raman intensity is mostly attributed to the absorption of the irradiated layer. The red shift of characteristic peak is assumed to be induced by the accumulation of isolated point defects [11]. In the waveguide region, a new Raman peak appears near ~781.5 cm^{-1} and the intensity of ~966.6 cm^{-1} mode is increased. The structure destruction of 4H-SiC and appearance of a new vibration mode are induced by high ion fluence during the ion irradiation process [26]. According to [7, 27], the variation of Raman spectra indicates that the ion irradiation process partially transforms 4H-SiC to 6H-SiC.

4. Summary

In conclusion, ridge waveguides in 4H-SiC single crystal have been fabricated by using C^{5+} ion irradiation and femtosecond laser ablation. The minimum propagation loss has been achieved by using the single-scan fs ablation and the maximum transmittance wavelength is at ~900 nm. The confocal μ-Raman spectra of the sample have shown microstructural changes in the waveguide region, suggesting a possible transition of 4H-SiC to 6H-SiC.

Acknowledgments

The work was carried out under the support by National Natural Science Foundation of China (No. U1332121) and the 973 Project (No. 2010CB832906) of China. The work was also supported by the Helmholz-Gemeinschaft Deutscher Forschungszentren (HGF-VH-NG-713) and Junta de Castilla y León (Project SA086A12-2).

#208123 - $15.00 USD Received 13 Mar 2014; revised 4 May 2014; accepted 6 May 2014; published 12 May 2014